Fabry-Perot interferometry with electron waves

1989 J. Phys.: Condens. Matter 1 9035

(http://iopscience.iop.org/0953-8984/1/45/026)

J. Phys.: Condens. Matter **1** (1989) 9035–9044. Printed in the UK

LETTER TO THE EDITOR

Fabry–Pérot interferometry with electron waves

C G Smith, M Pepper, H Ahmed, J E F Frost, D G Hasko, R Newbury, D C Peacock†, D A Ritchie and G A C Jones
Cavendish Laboratory, Madingley Road, Cambridge CB3 0HE, UK

Received 13 July 1989, in final form 18 August 1989

Abstract. We have constructed a gated device on a high mobility GaAs–GaAlAs heterostructure which acts as a ballistic channel within a resonant cavity defined by reflectors at each end. Both the channel width and the separation of the reflectors are smaller than the electron mean free path, such that when the channel is defined, oscillations in the resistance are observed as the distance between the reflectors is reduced. When the width of the channel is wide in comparison with the width of the voltage, or current probes, non-local voltage fluctuations result in the measured resistance going to zero. At intermediate channel widths the resistance oscillations are periodic in the separation of the reflectors with a period equal to half the Fermi wavelength. In this regime gradually changing the width enables one to calculate the change in phase of the electron wavefunction as it passes through a one-dimensional subband, this being found to be in good agreement with experiment. When the channel is very narrow, the resistance shows peaks of up to 200% which arise because of the overall quantisation imposed by the cavity.

The control of the width of an electron gas in a GaAs-GaAlAs heterostructure by means of a split Schottky gate is a convenient and fruitful method of investigating one dimensional (1D) transport. First demonstrated by Thornton *et al* (1986), the device can be used to investigate the 1D quantised levels (Berggren *et al* 1986) and their transport properties in a short ballistic structure (Wharam *et al* 1988a, van Wees *et al* 1988).

In our earlier work we were able to demonstrate that a range of interference phenomena can be observed by applying reflector potentials at the entrance to, and exit from, a narrow region defined by a split gate (Smith *et al* 1988, Wharam *et al* 1989a, Brown *et al* 1989). Under appropriate circumstances an electron standing wave can be established, and controlled in such structures which become quantum boxes when the reflecting potential is sufficiently strong.

In this work we present results obtained on a structure confining a narrow channel defined by split gates within a cavity established by a potential from confining gates at each end. We have observed interference in this structure as the sample length is changed demonstrating that the device behaves like a Fabry–Pérot interferometer based on electron waves.

The dimensions of the gate pattern, fabricated by electron beam lithography with a lift-off technique on top of an optically defined heterojunction Hall bar, are shown in

† Also at GEC Hirst Research Centre, East Lane, Wembley, Middlesex HA9 7PP, UK.

0953-8984/89/459035 + 10 $02.50

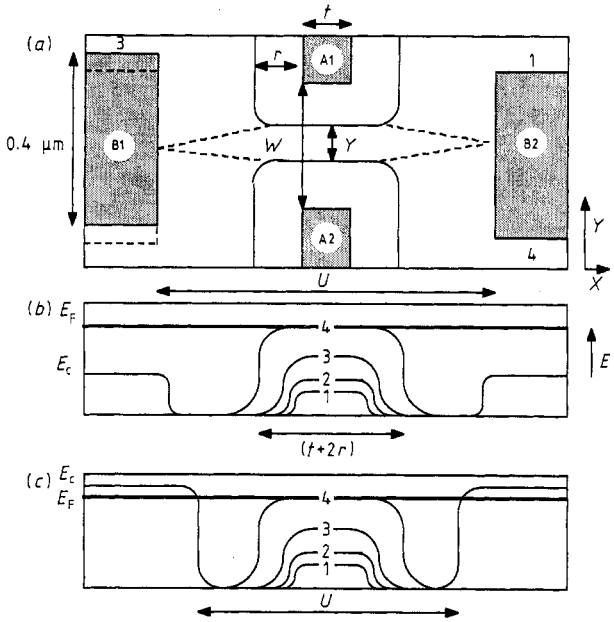

Figure 1. (*a*) Plan diagram of the metalisation at the centre of the Hall bar showing the four gates. The lithographically defined dimensions are $U = 1.02\ \mu m$, $W = 0.3\ \mu m$ and $t = 0.18\ \mu m$. r is a measure of the depletion width when a voltage is put on gate pair A1, A2, and Y is a measure of the conducting width of channel A. (*b*) The device was symmetrical apart from reflector B1 which was displaced by $0.1\ \mu m$ in the y direction. The band bending in the x direction when the reflectors B1 and B2 are grounded. The central region shows the energy levels for the 1D subbands in channel A with $k_{xn} = 0$ when $V_g(A) < -0.55$ V and $V_g(B) = 0$. (*c*) As for (*b*) for a more negative value of $V_g(B)$. The probe positions are labelled as 1, 2, 3 and 4.

figure 1(*a*). The details of the heterojunction are as follows: a superlattice buffer (AlAs 2.4 nm, GaAs 2.5 nm × 25) is grown on a semi-insulating substrate, followed by a 1 μm nominally undoped GaAs layer. Finally 20 nm of undoped AlGaAs is grown followed by 40 nm of AlGaAs doped at 10^{18} cm^{-3} with Si and topped by a 10 nm undoped GaAs capping layer. Because of charging effects during the electron-beam writing stage, the 60 nm thick AuPd gate-metal pattern is not perfectly symmetrical. The asymmetry is not important in consideration of the main physical result, but, as will be discussed, it does explain why probe 3 pinches off before the other probes. The two gates marked A1 and A2 were wired together as were the two marked B1 and B2. These two pairs of gates create a versatile device in which both the width and the length can be varied. To calculate how $V_g(A)$ (the gate voltage on probe A) is related to Y and $V_g(B)$ is related to U, where the lengths are defined in figure 1, we note that Y is independent of $V_g(B)$ and U is independent of $V_g(A)$. Grounding one pair of gates and sweeping the other leads to a variation of conductance against gate voltage for each gate pair. Although the resulting conductance trace shows peaks and plateaux as the gate voltage is swept, they are superimposed on a nearly linear background, which we assume is proportional to channel width (this is valid so long as there are more than three or more 1D subbands in channel A (Wharam *et al* 1989a)). We know that the width is zero when the device pinches off and that the width has the lithographically defined value minus a distance of the order of twice the separation between the gate and electron gas (0.07 μm in this case

(Wharam *et al* 1989b)) when the gates just deplete the carriers beneath them; we will then obtain

(i) width of channel A:

$$Y = [3.27 + V_g(\mathrm{A})]0.12\ \mu\mathrm{m}$$
$$\mathrm{d}Y/\mathrm{d}V_g(\mathrm{A}) = 120\ \mathrm{nm\ V^{-1}} \tag{1}$$

(ii) separation of reflectors:

$$U = [1.02 + (V_g(\mathrm{B}) + 0.55)0.19]\ \mu\mathrm{m}$$
$$\mathrm{d}U/\mathrm{d}V_g(\mathrm{B}) = 190\ \mathrm{nm\ V^{-1}}. \tag{2}$$

It should be noted that equation (1) was deduced in a slightly different manner, because the conductance against $V_g(\mathrm{A})$ was not linear over the whole range. The deviation occurred when the device was just defined and assumed to result from the short channel length combined with field spreading at either end. To obtain equation (1) the width was calculated from $Y = \lambda_f G e^2/h$ at two values of gate voltage over the linear region of conductance.

Our measurements were performed with the sample mounted in a top-loading dilution refrigerator operated at a base temperature of 30 mK. The resistance was recorded using a low-frequency AC technique with a constant current of not more than 1 nA. At these temperatures the electron mobility was $1.1 \times 10^6\ \mathrm{cm^2\ V^{-1}\ s^{-1}}$, with a carrier concentration of $3 \times 10^{11}\ \mathrm{cm^{-2}}$ which implies an electron mean free path of over 5 μm. As the longest device dimension is 1.02 μm, the electrons travel through it ballistically.

The experimental results show that four distinct modes of operation can be observed as the width of channel A is changed, these will now be discussed.

When the gate pair B1 and B2 are grounded and the pair A1 and A2 are swept to negative values, the normal broad plateaux of quantised resistance observed by Wharam *et al* (1988a) and van Wees *et al* (1988) at values of $R = h/2e^2n$ are not seen (figure 2, curve A). (Where n is the number of 1D subbands within channel A.) This is a consequence of the -0.5 V Schottky potential on the reflectors bending the conduction band, so setting up weak barriers which back-scatter the electrons at each end of the constriction. With an applied gate voltage of -0.55 V, resulting in a total gate voltage of -1.05 V, the electrons are completely depleted under the gates, i.e. the Schottky potential will be bending the conduction band up by $E_f/2$ (see figure 1(b)). The scattering of electrons off these potential barriers will in general reduce the transmission probability for electrons going through the split gate so that the plateaux associated with the nth 1D subbands will have a value (Fisher and Lee 1981) of,

$$R = h/2e^2\ \mathrm{Tr}(\mathbf{tt}^+) \tag{3}$$

where $\mathbf{t}$ is the N × N transmission matrix connecting the incident flux in the various channels on one side of the split gate with the outgoing flux in the channels on the other side. The dagger represents the Hermitian conjugate and Tr is the trace of the matrix. For the case of $n = 1$ equation (3) becomes $R = h/2e^2T$, where T is the transmission coefficient for that subband.

Resonance will occur when a standing wave is established by the waves that are back scattered through channel A. These will only exist for electrons with a small transverse

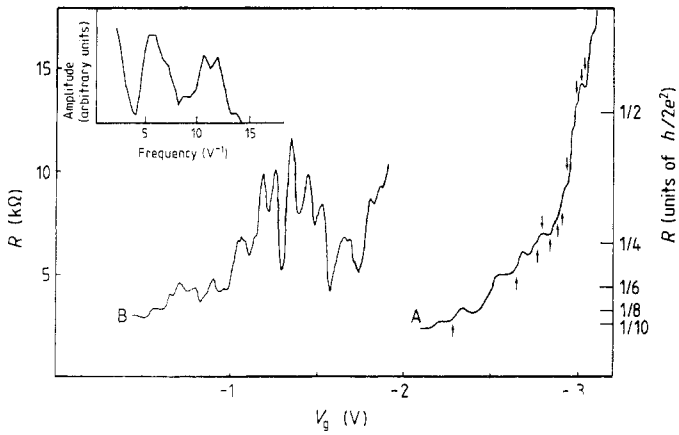

Figure 2. Curve A, plot of the resistance as $V_g(A)$ was varied while $V_g(B)$ was grounded. The arrows indicate the values of $V_g(A)$ for which equation (4) is valid for $n = 1$ (arrows above the trace) and $n = 2$ (arrows below the trace). The current was applied to probes 1 and 2 while the voltage was measured between probes 3 and 4. Curve B, variation of resistance against $V_g(B)$ for $V_g(A) = -2.45$ V ($Y = 98$ nm). The current was applied to probes 1 and 3, while the voltage was measured between probes 2 and 4. Inset: a Fourier power spectrum of trace B showing two peaks, one at 6 V^{-1} and the other at 12 V^{-1}.

momentum as those with larger values will be scattered out through the probes. The simplest condition for a standing wave is

$$k_x U + \varphi_n = m\pi \tag{4}$$

where m takes integer value 0, 1, 2, 3 . . . and φ_n is the difference in phase induced by the presence of the 1D channel when a wave in the wide 2D device passes through the nth 1D subband. Calculations show that there are 43 quantised levels along the channel, i.e. Fabry–Pérot states, when $U = 1$ μm and that their separation at the Fermi energy is 0.46 meV. As each φ_n depends on the width of channel A the transmission probability will oscillate, producing oscillations in the resistance in addition to the plateaux, as $V_g(A)$ is changed. Now to model how the resistance changes with the width of channel A we need to estimate φ_n and calculate how many subbands must be included in equation (4). A simple geometric argument for the return of electrons through the constriction, assuming that the length of the constriction increases by $2r$ when the width decreases by $2r$ (which has been shown to be valid by Wharam *et al* (1989a) and Smith *et al* (1989)), is given by

$$k_y < k_x Y/(U - L) \tag{5}$$

where $Y = (W - 2r)$ is the conducting width of the channel, $L = (t + 2r)$ its length and t its lithographically defined length (figure 1(*a*)). We note that in practice $k_x \approx k_f$. Therefore the electrons most likely to resonate will be those which have the smallest transverse momentum, given by

$$k_{yn} = \pi n/Y \tag{6}$$

where n is the 1D level index. Equations (5) and (6) enable one to calculate the minimum values of Y for which electrons in the nth subband in channel A will be reflected back

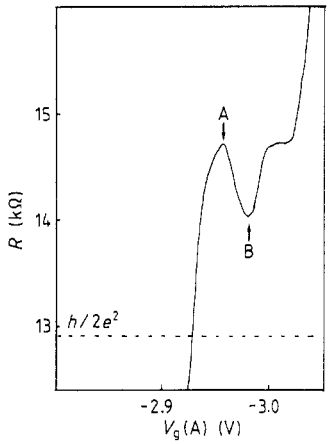

Figure 3. An expanded plot of R against $V_g(A)$ when the reflectors are fully defined with $V_g(B) = -0.706$ V ($U = 850$ nm). The current was applied to probes 1 and 3, while the voltage was measured between probes 2 and 4. The arrow A marks the minimum of T on the last plateau, while B marks the resonance.

through the channel. We find that $Y = 66$ nm for $n = 1$ and $Y = 190$ nm for $n = 2$ (for the experimental parameters $k_f = 108\ m^{-1}$ and $U = 0.85\ \mu m$).

We note that equation (5) does not take into account the focussing which occurs when an electron leaves the channel through a smooth existing potential. This results in the forward momentum being enhanced by the reduction in transverse momentum. The net effect is to relax the inequality defined by equation (5). It is this effect which results in transport being determined by the conservation of quantum number found by Wharam *et al* (1988b) using a structure consisting of the two slits in series.

We now calculate φ_n. The longitudinal momentum in the nth 1D subband is given by

$$(k_{xn})^2 = k_f^2 - (\pi n/Y)^2 \tag{7}$$

so in a channel of length L and width Y

$$\varphi_n = -L\pi^2 n^2/2k_f Y^2 \tag{8}$$

(we have assumed $k_{yn} \ll k_f$).

From equation (1) we can calculate the values of $V_g(A)$ for which equation (4) is valid for the $n = 1$ and 2 subbands and we mark them with arrows in curve A of figure 2. Obviously the oscillations due to the $n = 2$ level will die out as the channel narrows and equation (5) becomes invalid. The resistance should show dips at the values of $V_g(A)$ corresponding to waves resonating in the standing wave states set up between the reflectors. Although the fit is not perfect, it does explain why curve a in figure 2 shows oscillations as well as poorly quantised plateaux.

Figure 3 shows the shape of the last plateau as $V_g(A)$ is changed with the reflectors fully defined at a voltage of $V_g(B) = -0.706$ V ($U = 850$ nm). This four-terminal measurement shows the last plateau has a resistance that is $1.14\ h/2e^2$ and indicates the existence of a resonant state that causes a dip in this plateau (at the arrow marked B) which takes T from 0.875 to 0.927. The resonances are similar to that predicted by Kirczenow (1988) and Szafer and Stone (1989), only now the scattering is off the end reflectors and not off the corners at each end of channel A, as modelled in those papers.

To show the effect of changing the sample length, U, without changing the width of the channel, gate set A was kept at a constant voltage of -2.45 V (which corresponds to a width Y of 98 nm), and the voltage on the reflectors was swept. The results are shown in curve B of figure 2 and show that the resistance is now slowly increasing, but

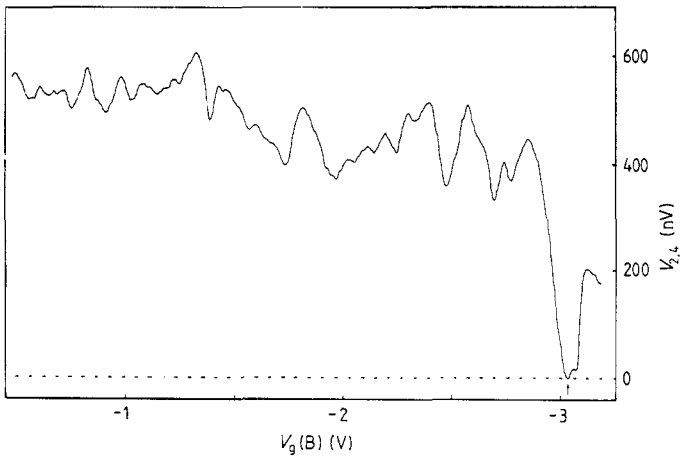

Figure 4. The variation of measured voltage between proves 2 and 4 with a current of 10 nA applied to proes 1 and 3. $V_g(A) = -1.003$ V ($Y = 0.27$ μm). The arrow marks the position at which the measured voltage goes to zero. The current through the device is unaltered at this point. The two-terminal resistance between the probes at $V_g(B) = -3.02$ V was $R_{2,3} = 18.8$ kΩ, $R_{3,1} = 18.8$ kΩ, $R_{1,4} = 4.4$ kΩ, $R_{4,2} = 2$ kΩ, $R_{1,2} = 4$ kΩ and $R_{3,4} = 19.4$ kΩ.

has large oscillations of up to 50% on a background resistance close to $h/4e^2$. In order to determine if these oscillations were of 'universal-conductance-fluctuation'-type arising from interference due to diffuse scattering, the magnetoresistance was investigated. With $V_g(A)$ at -2.45 V($Y = 98$ nm) and $V_g(B)$ at -0.720 V ($U = 848$ nm), the magnetic field was swept and it was found that with a $\boldsymbol{B}$ field perpendicular to the surface of the 2DEG any oscillations in resistance were at least a factor of 4 smaller than those seen when U is decreased, indicating that the length-dependent oscillations in zero field must be due to a resonance in the narrow channel as the first term in equation (4) is varied. With $\boldsymbol{B}$ in one direction the background change in R was constant while in the reverse field direction the background was linear and negative up to 0.4 T, and then constant with increasing magnetic field. This asymmetry reflects the asymmetry in the device shape with probe 3 being narrower than the others, in combination with the probes all being within an inelastic scattering length of each other causing $R(\boldsymbol{B}) \neq R(-\boldsymbol{B})$ (Büttiker 1988).

In figure 4 the voltage is measured between probes 2 and 4 while the current flows between 1 and 3, and a voltage $V_g(A) = -1.003$ V ($Y = 0.27$ μm) is applied to the gate set A. The trace shows how the measured voltage changes as $V_g(B)$ is varied, and alters the sample length; in particular the measured voltage drops to zero at the position marked by the arrow. This effect was generally observed for values of $V_g(A)$ consistent with a wide sample and occurs when one of the probe widths comes close to pinch-off, for example when $V_g(B) = -3.02$ V, in figure 4, the two-terminal resistance was measured between all the voltage probes in turn. At this gate voltage probes 1, 2, and 4 have a low resistance of (2–4) kΩ, but probe 3 is nearly pinched off and has a resistance close to $h/2e^2$, suggesting that there is only one subband in that probe (this is a result of the previously mentioned asymmetric shape of the device). The wider probes are of the order 120 nm when $R = 0$. Therefore these anomalous voltage oscillations only occur when the channel width is large compared to all the probe widths and one of the probes

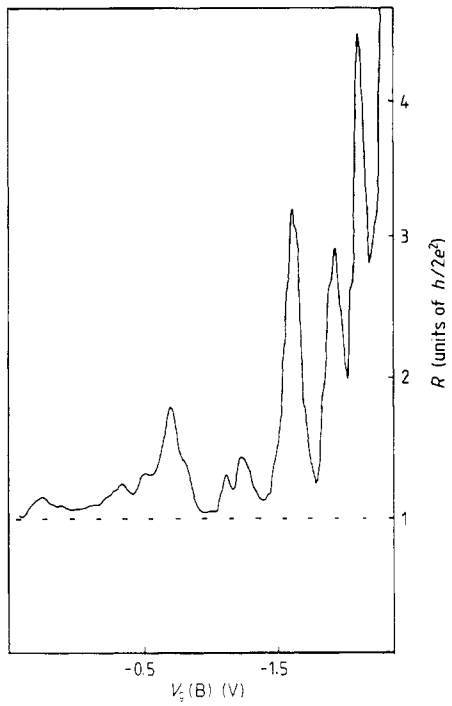

Figure 5. The variation of resistance with V_g(B) for V_g(A) = −2.803 V (Y = 56 nm). The current is applied to probes 1 and 3 while the voltage is measured between 2 and 4.

is close to pinch-off. As the probes are all within an inelastic scattering legnth of each other non-local effects will dominate. In this regime it is possible that the states that leave the current probes do not have a large overlap integral with the states in the voltage probes, i.e. the voltage probes have become weakly coupled. Büttiker (1988) suggests that for weakly coupled probes measured in a four-terminal fashion, a negative voltage can be measured across the voltage probes when a positive voltage is applied to adjacent current probes. We note that this trace is not periodic in V_g(B), due to resonance, as channel A is too wide at 270 nm. The observation of a periodicity requires a narrow channel with few subbands so that higher order phase terms are not present.

To optimise the device dimensions to obtain Fabry–Pérot behaviour with electron waves, one might initially think that channel A should be of such a width that it contains just one 1D subband. In this regime only the phase term will exist in equation (4), and the resistance of the channel will dominate reducing the effects of the non-local voltage fluctuations from the probes. Figure 5 shows the variation in resistance for the case when the constriction is nearly completely pinched off with V_g(A) = −2.803 V (Y = 56 nm). The current flows between probes 1 and 3 whilst the voltage is measured between 2 and 4 as V_g(B) is varied. The resistance is now close to $h/2e^2$ indicating that only one 1D subband in channel A is occupied, but there are now peaks at which the resistance increases by up to a factor of 3 at certain values of V_g(B). The peaks in the resistance appear to always rise from a base value of $h/2e^2$ and they result from the further quantisation of the system due to the reflectors. At certain values of U there is not an allowed eigenstate for electrons with the Fermi momentum so resistance rises sharply. Curve B of figure 2 illustrates the length-dependent oscillations when only two subbands are occupied, the inset to this figure shows the Fourier power spectrum and it is clear that two frequencies are present. The dominant periodicity arises from standing waves

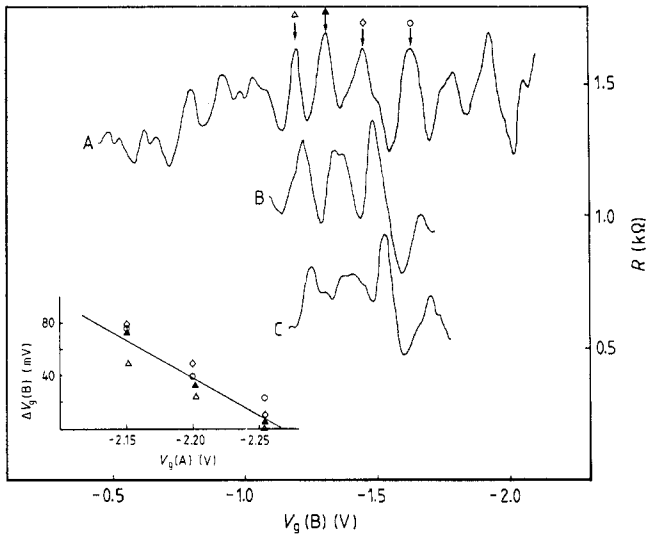

Figure 6. The resistance measured with current in contacts 1 and 3 and voltage between probes 2 and 4 for varying V_g(B). Curve A, V_g(A) = −2.255 V (Y = 122 nm); curve B V_g(A) = −2.202 V (Y = 128 nm); curve C, V_g(A) = −2.157 V (133 nm). For clarity curve B has been displaced down by 200 Ω while curve C has been displaced down by 400 Ω. As the channel is narrowed the peaks marked by the arrow move to lower gate voltages. Inset: the shift in V_g(B) for various V_g(A) for the peaks marked by the arrows. A best fit line was computed by averaging the shift for all the peaks marked, and is drawn on the inset.

in the entire cavity and the other is due to a standing wave arising from a reflection at the entrance to, or exit from, the narrow channel so halving the period. The half-resonance effect only occurs when the number of occupied subbands is few and the difference between Fermi energy and ground-state energy in the channel is small.

To optimise the device shape for the Fabry–Pérot condition we increased the channel width to reduce the reflections off the subbands in the channel, but kept it narrower than the voltage probes. In figure 6 the four-terminal resistance is shown for the sample with the current passed between contacts 1 and 3 and the voltage measured between 2 and 4. For the sweep in curve A the voltage on the gate pair A1, A2 was −2.255 V (Y = 122 nm), while that on the reflectors was varied. Again the resistance oscillates around a mean value by up to 30%, but now the peaks are nearly periodic, as can be seen from figure 7, which shows the Fourier transform power spectrum of curve A in figure 6 with a strong peak at a frequency of 7 V^{-1}. The peak corresponds to a periodic oscillation in V_g(B) of 143 mV, which converts into a variation of sample length (using equation (2)) of 27 nm. As there are four gates at a negative voltage within close proximity of each other when the conducting channel and barriers are defined, the carrier concentration within the device is not the same as when the gates are grounded. For this reason a plot of magneto-resistance was made and the resulting Shubnikov–de Haas oscillations used to calculate the carrier concentration. The current was fed in contacts 1 and 3, and the voltage measured between 2 and 4, with gates V_g(A) = −0.55 V (Y = 0.3 μm) and gates V_g(B) = −0.98 V (U = 798 nm). The obtained carrier concentration was reduced below the value for grounded gates and corresponded to a Fermi wavelength of 55 nm. Thus the periodicity in resistance with U fits well with a maximum occurring every time the device length changes by one half Fermi wave length.

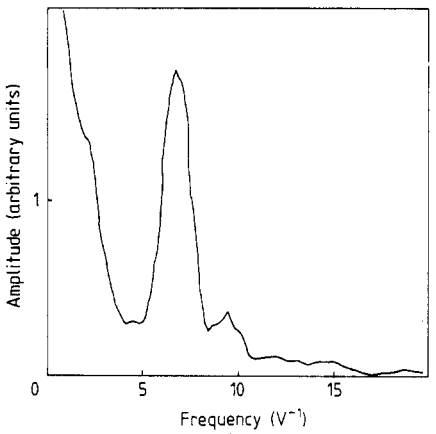

Figure 7. The Fourier power spectrum of curve A in figure 6. The amplitude is plotted against the frequency in V^{-1}.

Returning to figure 6, the traces A, B and C show how narrowing the width of the channel by a small amount causes the resonant structure to shift to lower values of gate voltage as the phase term φ_n in equation (3) changes. From equation (7) we find

$$d\varphi/dr = 2\pi^2 n^2 L/k_f Y^3 \tag{9}$$

and combining this with equation (1) gives

$$d\varphi = (2\pi^2 n^2 L/k_f Y^3) \times 63\ \text{nm} \times \Delta V_g(\text{A}) \tag{10}$$

where $\Delta V_g(\text{A})$ is the change in voltage on the channel gates. The measured shift in phase will be given by

$$d\varphi = -k_f \times 0.22\ \mu\text{m} \times \Delta V_g(B) \tag{11}$$

where $\Delta V_g(\text{B})$ is the shift in the position of any given peak for a given change $\Delta V_g(\text{A})$. This was calculated from the slope of the inset to figure 6. For $k_f = 100\ \text{m}^{-1}$ (obtained from the Shubnikov–de Haas effect) and $\Delta V_g(\text{A}) = -0.095$ V the measured phase shift from equation (11) is 1.32 radians while that calculated from equation (10) is 0.26 radians for $n = 1$ and 1.02 radians for $n = 2$. Therefore these peaks are associated with the second subband. The discrepancy between the measured and calculated values can be accounted for by a 10% error in our estimate of Y. It remains to be explained why the $n = 2$ subband dominates the phase shift. However, as discussed earlier, the higher subbands with greater transverse momentum are unlikely to be reflected back through the channel. On the other hand the higher subbands have a higher density of states at the Fermi energy and therefore will give a greater contribution to the resonance and so dominate the oscillations. The net effect appears to favour $n = 2$ rather than $n = 1$ or $n > 2$.

In conclusion, we have made a device in which electron transport is ballistic and whose width and length can be separately varied. By setting up reflecting barriers at each end of a split gate the normal quantised plateau in resistance are removed by a variation in transmission coefficient. The resistance was found to oscillate as the length of the device is changed; when the channel is narrow, peaks appear on a constant background which can be up to three times the original resistance and they occur when there is a bound level between the end reflectors. In this regime the device behaves in a similar manner to that calculated by Fernando Sols *et al* (1989) for a T-shaped structure.

When the channel is wide the voltage measured for constant current oscillates, with the device length having sharp dips which take the measured resistance to zero at certain reflector separations; this can be explained in terms of the non-local nature of the voltage probes, which are all within a phase coherence length of each other. At certain intermediate channel widths, when the localised waves match into the lowest 1D subbands without reflection, the resistance oscillates periodically with length having a period of a half Fermi wavelength. It is possible to observe how the $n = 2$ subband changes the phase of the electron wavefunction as it passes through channel A. Thus, the device is behaving like a Fabry–Pérot interferometer with a variable phase shifter provided by the variable-width channel.

References

Berggren K F, Thornton T J, Pepper M, Ahmed A, Andrews D and Davies G 1986 *Phys. Rev. Lett.* **56** 1198

Brown R, Smith C G, Pepper M, Ahmed H, Frost J E F, Hasko D G, Peacock D C, Ritchie D A and Jones G A C 1989 *J. Phys.: Condens. Matter* **1** 6291

Büttiker M 1988 *IBM J. Res. Dev.* **32** 317

Sols F, Macucci M, Ravaioli U and Hess K 1989 *Appl. Phys. Lett.* **54** 350

Fisher D S and Lee P A 1981 *Phys. Rev.* B **23** 6851

Kirczenow G 1988 *Solid State Commun.* **68** 715

Smith C G, Pepper M, Ahmed H, Frost J E F, Hasko D G, Peacock D C, Ritchie D A and Jones G A C 1988 *J. Phys. C: Solid State Phys.* **21** L893–8

Smith C G, Pepper M, Newbury R, Ahmed H, Hasko D G, Peacock D C, Frost J E F, Ritchie D A, Jones G A C and Hill G 1989 *J. Phys.: Condens. Matter* **1** 6763

Szafer A and Stone A D 1989 *Phys. Rev. Lett.* **62** 300

Thronton T J, Pepper M, Ahmed H, Andrews D and Davies G J 1986 *Phys. Rev. Lett.* **56** 1198

van Wees B J, van Houten H, Beenakker C W J, Williamson J G, Kowenhoven L P, van der Marel D, Foxon C T 1988 *Phys. Rev. Lett.* **60** 848

Wharam D A, Thornton T J, Newbury R, Pepper M, Ahmed H, Frost J E F, Hasko D G, Richie D A and Jones G A C 1988a *J. Phys. C: Solid State Phys.* **21** L209

Wharam D A, Pepper M, Newbury R, Ahmed H, Hasko D G, Frost J E F, Peacock D C, Ritchie D A and Jones G A C 1988b *J. Phys. C: Solid State Phys.* **21** L893

Wharam D A, Pepper M, Newbury R, Ahmed H, Hasko D G, Peacock D C, Frost J E F, Richie D A and Jones G A C 1989a *J. Phys. Condens. Matter* **1** 3369

Wharam D A, Ekenburg U, Pepper M, Hasko D G, Ahmed H, Frost J E F, Ritchie D A, Peacock D C and Jones G A C 1989b *Phys. Rev.* B **39** 6283